

# Rotational Entropy Driven Separation of Alkane/Isoalkane Mixtures in Zeolite Cages\*\*

Joeri F. M. Denayer,\* Refik A. Ocakoglu, Ilbige C. Arik, Christine E. A. Kirschhock, Johan A. Martens, and Gino V. Baron

Molecular separation and purification processes are key operations in chemical industry.<sup>[1]</sup> High separation power is obtained in separation processes that are based on adsorption in zeolite micropores.<sup>[2]</sup> Molecular separation on zeolites can originate from several types of interactions. Electrostatic interactions are responsible for the selective adsorption of nitrogen from air, in the drying of gases, and the removal of polar impurities such as carbon monoxide, mercaptans, or organic chlorides from gases and liquids.<sup>[3,4]</sup> Shape-selectivity separation arises from the subtle matching of the size and shape of guest molecules and zeolite micropores.<sup>[5]</sup> Generally, adsorption and diffusion of more-bulky molecules is restricted by the small pore size. To boost octane ratings in gasoline, linear alkanes are sieved from the more-bulky branched alkanes by using narrow-pore molecular sieves.<sup>[5,6]</sup> Herein we take advantage of cage structures offered by special zeolite adsorbents such as MCM-22. The retention of alkane molecules in MCM-22 is governed by rotational freedom in its cages. The preferential adsorption of isopentane over *n*-pentane in MCM-22 zeolite is a first example of such rotational entropy driven separation.

The adsorptive separation power of a solid is determined by the equilibrium constants of adsorption of the molecules of interest. These equilibrium constants in turn relate to the adsorption enthalpy (the energetic interaction between the molecule and the host environment of the zeolite pore) and the adsorption entropy (the loss of freedom that a molecule experiences in the transition from the gaseous state to the adsorbed state). Depending on the strength of interaction and the pore type, molecules that are confined in zeolite pores lose rotational and translational freedom.<sup>[7]</sup> In large tubular pores, at least one degree of translational freedom is retained along the axis of the pore. However, in zeolite cages, translational freedom is severely reduced, hence the contri-

bution of molecular rotation to the entropy becomes an essential factor in the relative adsorption equilibria of molecules of different sizes and shapes.<sup>[8]</sup>

The ability of a molecule to rotate in a cage can be estimated by comparing the radius of gyration of its van der Waals volume  $R_g$ , which assumes rotation around the centre of mass, to the radius  $R_c$  of the largest sphere that fits into the van der Waals contour of the cage or pore. Minimal loss of rotational entropy is combined with maximal energetic interactions when the sphere that circumscribes the rotational motion of the molecule matches the internal surface of the cage; that is, when the radius ratio  $R_g/R_c$  equals unity. The equilibrium adsorption properties of linear and branched alkanes on zeolites that comprise cages or tubular pores were determined to investigate this effect. Isoalkanes, with their shorter carbon backbone, have a smaller radius of gyration and a more spherical shape than their linear counterparts, thus they might rotate more easily in zeolite cages which could lead to their preferential adsorption.

Mordenite and ZSM-22 have one-dimensional pores with dimensions of  $0.70 \times 0.65 \text{ nm}^2$  and  $0.45 \times 0.55 \text{ nm}^2$ , respectively (Figure 1). NaY contains spherical supercages with a diameter of 1.23 nm that are connected by windows of 0.73 nm (Figure 1). MCM-22 contains large nonspherical supercages of 1.82-nm height that are accessible through 10-ring apertures of  $0.40 \times 0.54 \text{ nm}^2$  (Figure 1).<sup>[9]</sup> The top and bottom part of the MCM-22 supercages are pockets of 0.7–

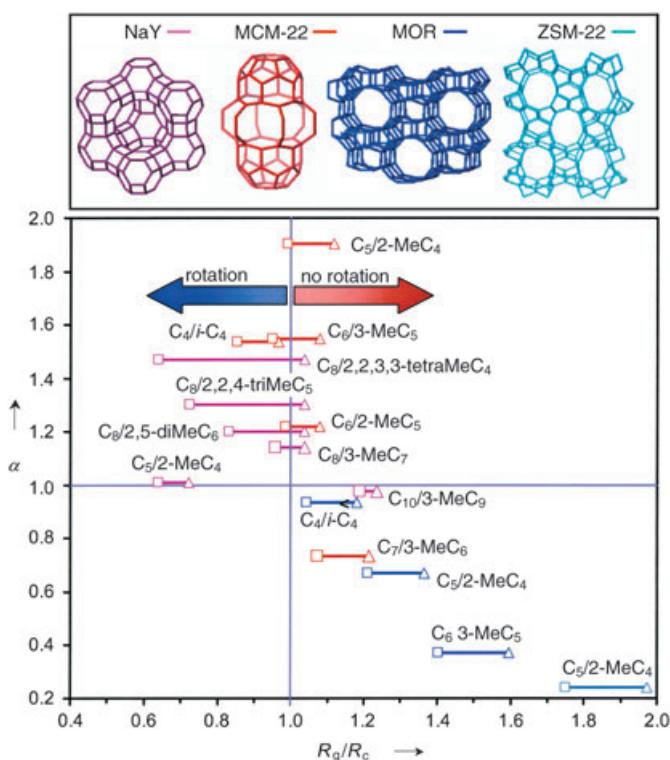


**Figure 1.** Ratio ( $\alpha$ ) of low coverage adsorption constants of branched and linear alkanes on MCM-22, NaY, Mordenite (MOR), and ZSM-22 plotted against the radius ratio  $R_g/R_c$ .  $R_{g(i)}$  and  $R_{g(n)}$  represent the radii of gyration of the iso- and *n*-alkanes, respectively, and  $R_c$  represents the radius of the largest sphere that fits into the zeolite cage.  $\Delta$  corresponds to  $R_{g(i)}/R_c$  and  $\square$  corresponds to  $R_{g(n)}/R_c$ .

[\*] Dr. J. F. M. Denayer, Dr. R. A. Ocakoglu, I. C. Arik, Prof. Dr. G. V. Baron  
Department of Chemical Engineering  
Vrije Universiteit Brussel  
Pleinlaan 2, 1050 Brussel (Belgium)  
Fax: (+32) 2-629-3248  
E-mail: joeri.denayer@vub.ac.be

Dr. C. E. A. Kirschhock, Prof. Dr. J. A. Martens  
Center for Surface Chemistry and Catalysis  
Katholieke Universiteit Leuven  
Kasteelpark Arenberg 23, 3001 Leuven (Belgium)

[\*\*] J.F.M.D. and C.E.A.K. are grateful to FWO Vlaanderen for post-doctoral research fellowships. J.A.M. acknowledges the Flemish Government for supporting a Concerted Research Action on the understanding of the active site in catalysis.

0.8 nm in diameter, whereas the broadened central part of this supercage, which resembles a squeezed ellipsoidal cage, is capable of hosting larger molecules. MCM-22 and related materials show interesting adsorption, diffusion, and catalytic properties.<sup>[10–15]</sup>

Separation factors ( $\alpha$ ), which are computed as the ratios of the Henry adsorption constants for branched over linear alkanes, are plotted against radius ratios  $R_g/R_c$  in Figure 1. For Mordenite and ZSM-22, separation factors of less than 1 are observed which indicates that the linear alkanes are adsorbed preferentially. *n*-Alkanes and isoalkanes have a radius of gyration which is larger than the largest sphere that fits in the tubular pores of Mordenite and ZSM-22, so rotational freedom is severely restricted for both types of molecules. For *n*-butane/isobutane on Mordenite, the preference for the linear alkane is the least pronounced. The radius of gyration of isobutane is only slightly larger than  $R_c$  for this zeolite.

With MCM-22 and NaY, a reversal of the normal order of selectivity is observed for several *n*-alkane/isoalkane couples. A selective adsorption of the isoalkane is observed for isobutane, 2-methylbutane, and 2- and 3-methylpentane on MCM-22. The largest separation factor (1.9) is obtained for the *n*-pentane/2-methylbutane couple. The sphere circumscribing the rotation of 2-methylbutane neatly fits into the pocket of the upper and lower parts of the MCM-22 supercage (Figure 2a), whereas *n*-pentane is unable to rotate in that volume. 2-Methylpentane and 3-methylpentane are too large to enable rotation in the pockets of MCM-22, but their gyration spheres fit into the central part of the MCM-22 supercage (Figure 2b).

A pronounced selectivity in favor of the isoalkane is also observed with 2,2,3,3-tetramethylbutane, 2,2,4-trimethylpentane, 2,5-dimethylhexane, and 3-methylheptane on NaY (Figure 1). *n*-Octane is a little too large to rotate freely in the NaY supercages, whereas its isomers retain rotational freedom. The selectivity becomes more pronounced when the difference in  $R_g$  between the branched and linear alkanes increases (Figure 1).

With smaller alkanes (e.g. *n*-pentane/2-methylbutane on NaY), the rotation of the *n*-alkane is barely hampered and the differences in rotational freedom between linear and

branched alkanes are minor (Figure 1). Consequently, only a low selectivity for the branched alkane is observed. Similarly, when the isoalkane becomes too large to rotate in the zeolite cage, it loses its advantage in rotational freedom and selectivity in favor of the linear chain is observed (e.g. *n*-decane/3-methylnonane on NaY and *n*-heptane/3-methylhexane on MCM-22).

Differences in rotational freedom between molecules are reflected in the adsorption entropy. In Figure 3, the adsorption entropy is plotted as a function of adsorption enthalpy for

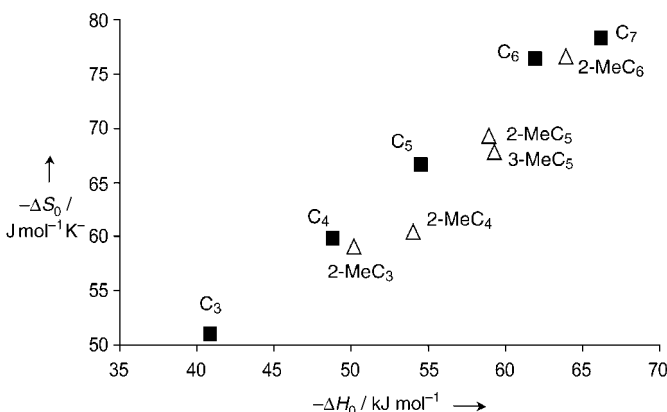


**Figure 3.** Compensation plot between the adsorption entropy and enthalpy for  $C_3$ – $C_7$  *n*-alkanes (■) and their methyl-branched isomers (Δ) on zeolite MCM-22.

MCM-22. For a branched molecule to have a higher Henry adsorption constant than its linear isomer, it needs to have a combination of adsorption enthalpy and entropy that results in a lower Gibbs free energy of adsorption. 2-Methylbutane, 2-methylpentane, and 3-methylpentane obviously lose much less entropy in the adsorbed state relative to their linear isomers. For example, the entropy loss of 3-methylpentane is lower than that of *n*-hexane by  $9.0 \text{ J mol}^{-1} \text{ K}^{-1}$ . Consequently, these isoalkanes are adsorbed preferentially over their linear isomers despite their less favorable adsorption enthalpy. For the *n*-heptane/2-methylhexane couple, the difference in adsorption entropy is only  $1.7 \text{ J mol}^{-1} \text{ K}^{-1}$  as a result of the restricted rotation of 2-methylhexane. Compared to *n*-butane, isobutane has a slightly higher adsorption enthalpy (*n*-butane:  $48.8 \text{ kJ mol}^{-1}$ ; isobutane:  $50.1 \text{ kJ mol}^{-1}$ ) which is explained by a better agreement between the shape of isobutane and the pockets of MCM-22. Moreover, isobutane has a less-negative adsorption entropy, which indicates that this molecule loses less freedom in the adsorbed state than its linear isomer although it is more strongly interacting.

By exploiting rotational entropy effects, separation patterns that are different from those found typically

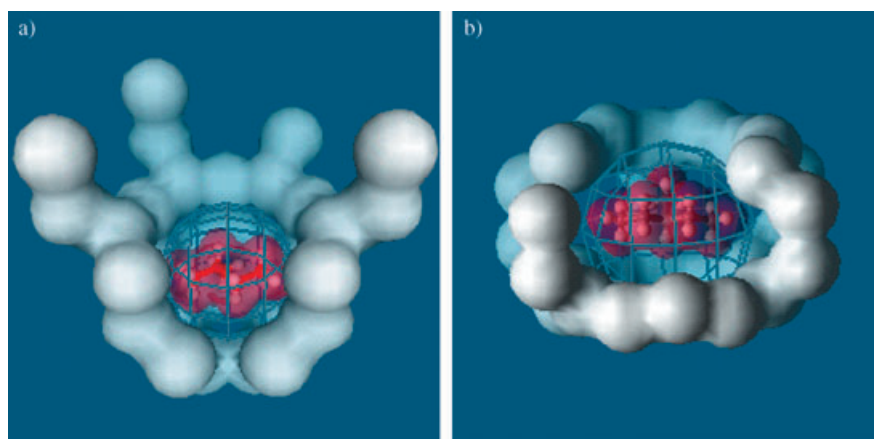


**Figure 2.** a) A molecule of 2-methylbutane with its radius of gyration in the lobe of the MCM-22 supercage and b) 3-methylpentane in the central part of the MCM-22 supercage.

can be obtained. Figure 4, a–c, show the chromatograms obtained after injection of mixtures of linear and branched alkanes on zeolite columns. With Mordenite, 2-methylbutane elutes first from the column followed by *n*-pentane (Fig-

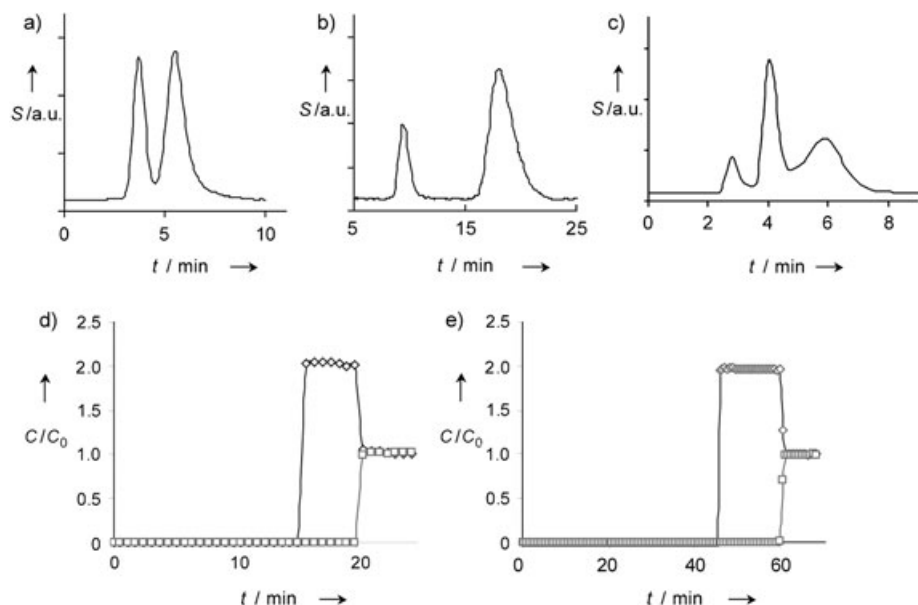


**Figure 4.** a–c) Chromatograms of *n*-alkane/isoalkane mixtures obtained on zeolite columns at 200 °C ( $S$  = detector signal): a) separation of *n*-pentane and 2-methylbutane on Mordenite, b) separation of *n*-pentane and 2-methylbutane on MCM-22, and c) separation of *n*-hexane, 3-methylpentane, and 2,2-dimethylbutane on MCM-22. d) and e) Breakthrough profiles obtained on an MCM-22 column at 130 °C with a total hydrocarbon pressure of 0.2 bar ( $C$  = concentration): d) equimolar *n*-pentane ( $\diamond$ )/2-methylbutane ( $\square$ ) mixture, e) equimolar *n*-butane ( $\diamond$ )/isobutane ( $\square$ ) mixture.

ure 4a). This order of affinity is common to zeolite types studied previously.<sup>[16–18]</sup> On an MCM-22 column, the retention order is reversed as a result of the higher adsorption equilibrium constant of the branched alkane (Figure 4b). Even more remarkable is the separation of a ternary mixture of differently branched alkanes on MCM-22 (Figure 4c). *n*-Hexane elutes between 2-methylpentane and 2,2-dimethylbutane; the bulkiest dibranched isomer is too large to enter the MCM-22 supercages and therefore elutes first.<sup>[10–12]</sup> Figure 4, d and e, show breakthrough profiles for *n*-pentane/2-methylbutane and *n*-butane/isobutane mixtures separated on an MCM-22 column. The branched alkanes are selectively trapped inside the MCM-22 pores and displace the adsorbed linear alkanes along the column profile until the composition inside the pores reaches thermodynamical equilibrium. Also under these conditions whereby the MCM-22 pores are saturated with molecules, a good separation with selectivity for the branched alkanes is found.

Recent molecular modeling studies demonstrated that a selective uptake of isoalkanes from *n*-isoalkane mixtures might occur at high pressures and high zeolite loadings in zeolites with tubular pores of 0.6–0.75 nm because more of these shorter isoalkanes can be packed into a single file relative to the linear chains.<sup>[19,20]</sup> The effect observed in the present work already occurs at low pressure with isolated molecules adsorbed in zeolite cages rather than in tubular

pores and does not invoke molecular packing phenomena. To investigate whether the preference of MCM-22 for mono-branched alkanes extends beyond the low-coverage domain, where adsorbed molecules are isolated from each other, the adsorption selectivity for a *n*-pentane/2-methylbutane mixture was determined in the liquid phase at complete saturation of the pores of MCM-22. Also under these conditions, 2-methylbutane was selectively adsorbed with a separation factor between 2-methylbutane and *n*-pentane of 1.4.

In summary, a new principle for molecular separation based on differences in molecular rotation in zeolite cages has been introduced. Rotational entropy driven separation could be useful in the separation of structural isomers, such as *n*- and isoalkanes, aromatic compounds, or possibly other mixtures of differently shaped molecules. The recent development of new porous materials with much larger cavities than the ones investigated here opens perspectives for new, entropic-based separations with larger molecules.<sup>[21]</sup>

## Experimental Section

MCM-22 (Si:Al 30) was synthesized according to the method described in US Patent 5146029.<sup>[22]</sup> ZSM-22 (Si:Al 30) was prepared according to the procedure reported by Ernst et al.<sup>[23]</sup> NaY (CBV100, Si:Al 2.5) and Mordenite (CP-500C-11, Si:Al 5.5) were purchased from Zeolyst. Chromatographic and breakthrough experiments

were performed to study the adsorption properties of these adsorbents.<sup>[2]</sup> Adsorption equilibrium Henry constants were calculated from the first moment of the chromatographic response curves. Linearity of the experiments and absence of diffusion limitations was confirmed with different amounts of injection and by using different carrier flow rates. A detailed explanation of the experimental setup and procedure can be found elsewhere.<sup>[24]</sup> From the temperature dependence of the Henry coefficients ( $K'$ ), the adsorption enthalpy ( $\Delta H_0$ ) is calculated according to Equation (1). The adsorption entropy ( $\Delta S_0$ ) is calculated by using Equation (2)<sup>[20]</sup> and Equation (3), wherein  $\rho_c$  is the crystal density of the zeolite,  $T$  corresponds to the temperature (K), and  $R$  is the universal gas constant.

$$K' = K'_0 e^{\frac{-\Delta H_0}{RT}} \quad (1)$$

$$\Delta G_0 = -RT \ln(K' \rho_c RT) \quad (2)$$

$$\Delta S_0 = \frac{\Delta H_0 - \Delta G_0}{T} \quad (3)$$

The adsorption selectivity in the liquid phase was determined by using a static method at room temperature.<sup>[25]</sup>

Received: February 19, 2004

Revised: October 4, 2004 [Z54058]

**Keywords:** adsorption · alkanes · isomers · thermodynamics · zeolites

- [1] J. M. Coulson, J. F. Richardson, J. R. Backhurst, J. H. Harker, *Chemical Engineering*, Vol. 2, Pergamon, Oxford, **1991**, pp. 735.
- [2] D. M. Ruthven, *Principles of Adsorption and Adsorption Processes*, Wiley, New York, **1984**.
- [3] J. D. Sherman, *Proc. Natl. Acad. Sci. USA* **1999**, *96*, 3471–3478.
- [4] R. A. Meyers, *Handbook of Petroleum Refining Processes*, 2nd ed., McGraw-Hill, New York, **1996**, Chapter 10.6.
- [5] N. Y. Chen, W. E. Garwood, F. G. Dwyer, *Shape-Selective Catalysis in Industrial Applications*, Marcel Dekker, New York, **1989**.
- [6] S. Kulprathipanja, R. W. Neuzil, US Patent 4 445 444, **1984**, UOP.
- [7] P. S. Rallabandi, D. M. Ford, *AIChE J.* **2000**, *46*, 99–109.
- [8] R. Mukhopadhyay, A. Sayeed, M. N. Rao, A. V. Anilkumar, S. Mitra, S. Yashonath, S. L. Chaplot, *Chem. Phys.* **2003**, *292*, 217–222.
- [9] S. L. Lawton, M. E. Leonowicz, R. D. Partridge, P. Chu, M. K. Rubin, *Microporous Mesoporous Mater.* **1998**, *23*, 109–117.
- [10] H. Du, M. Kalyanaraman, M. A. Cambor, D. H. Olson, *Microporous Mesoporous Mater.* **2000**, *40*, 305–312.
- [11] W. J. Roth, C. T. Kresge, J. C. Vartuli, M. E. Leonowicz, A. S. Fung, S. B. McCullen, *Stud. Surf. Sci. Catal.* **1995**, *94*, 301–308.
- [12] A. Corma, C. R. Catlow, G. Sastre, *J. Phys. Chem. B* **1998**, *102*, 7085–7090.
- [13] R. Ravishanker, D. Bhattacharya, N. E. Jacob, S. Sivasanker, *Microporous Mater.* **1995**, *4*, 83–93.
- [14] F. Eder, Y. He, G. Nivarthi, J. A. Lercher, *Recl. Trav. Chim. Pays-Bas* **1996**, *115*, 531–593.
- [15] A. Corma, V. Fornes, S. B. Pergher, T. L. M. Maesen, J. G. Buglas, *Nature* **1998**, *396*, 353–356.
- [16] K. Huddersman, M. Klimczyk, *J. Chem. Soc. Faraday Trans.* **1996**, *92*, 143–147.
- [17] L. Boulicaut, S. Brandani, D. M. Ruthven, *Microporous Mesoporous Mater.* **1998**, *25*, 81–93.
- [18] J. F. M. Denayer, G. V. Baron, P. A. Jacobs, J. A. Martens, *J. Phys. Chem. B* **1998**, *102*, 3077–3081.
- [19] M. Schenk, S. Calero, T. L. M. Maesen, L. L. van Benthem, M. G. Verbeek, B. Smit, *Angew. Chem.* **2002**, *114*, 2609–2612; *Angew. Chem. Int. Ed.* **2002**, *41*, 2499–2502.
- [20] M. Schenk, S. Calero, T. L. M. Maesen, T. J. H. Vlucht, L. L. van Benthem, M. G. Verbeek, B. Schnell, B. Smit, *J. Catal.* **2003**, *214*, 88–99.
- [21] J. L. C. Roswell, O. M. Yaghi, *Microporous Mesoporous Mater.* **2004**, *73*, 3–14.
- [22] J. R. A. Huss, C. Chu, A. Husain, R. G. Bundens, K. M. Keville (Mobil Oil Corp., US), US Patent 5 146 029.
- [23] S. Ernst, J. Weitkamp, J. A. Martens, P. A. Jacobs, *Appl. Catal.* **1989**, *48*, 137–148.
- [24] A. R. Ocakoglu, J. F. M. Denayer, G. B. Marin, J. A. Martens, G. V. Baron, *J. Phys. Chem. B* **2003**, *107*, 398–406.
- [25] J. F. M. Denayer, K. De Meyer, J. A. Martens, G. V. Baron, *Angew. Chem.* **2003**, *115*, 2880–2883; *Angew. Chem. Int. Ed.* **2003**, *42*, 2774–2777.